J Mater Sci (2007) 42:7311–7315
DOI 10.1007/s10853-007-1578-x

Modified directed melt nitridation of pure aluminum block using magnesium as an external dopant

Shengli Jin · Yawei Li · Yuanbing Li · Lei Zhao · Liu Xiaohua · Jing Liu · Zeya Li

Received: 17 September 2006 / Accepted: 2 February 2007 / Published online: 10 May 2007

Abstract Modified directed melt nitridation of pure Al block was investigated by using magnesium as an external dopant at 1373–1573 K during the flowing high pure N_2. The products were characterized using optical microscope, X-ray diffractometer, scanning electron microscope and electron probe microanalysis techniques. Experimental results show that it is a lower costs way to synthesize AlN matrix or Al matrix materials by modified directed melt nitridation through adapting proper processing parameters. The weight gain rate increased significantly with the treating temperature and Mg content. Apparent activation energy of 208.7 KJ/mole was obtained in terms of the reaction rate involving nitridation, evaporation and transportation. AlN reinforced Al matrix material was fabricated with less Mg and AlN particles were enriched in the top part of the product with distinct boundary to the bottom Al. however, when the content of Mg was up to 10 wt% and treated at higher treating temperature, AlN phase dominated in the product with a relative looser structure.

S. Jin (✉) · Y. Li · Y. Li · L. Zhao · L. Xiaohua · J. Liu
State Key Laboratory Breeding Base of Refractories and Ceramics, Wuhan University of Science and Technology, No. 947 Heping Ave, Wuhan 430081, China
e-mail: kingsle_jin@yahoo.com.cn

Z. Li
Shanghai Baosteel Institute, Shanghai 201900, China

Introduction

At the beginning of 1980's, directed melt oxidation of Al alloy into Al_2O_3/Al composites, was originally reported by Newkirk et al [1]. This method includes the ability to tailor the composite properties by selecting different processing parameters, such as matrix compositions, treating temperatures; also low costs and especially the elimination of densification shrinkage. It is promising to make very large ceramic bodies. A related process, directed melt nitridation was adopted to fabricate AlN/Al composite from Al alloys, which attracts much interest of material researchers recently [2]. As to the directed melt nitridation of Al alloy, Mg is necessary to keep fresh Al meeting with N_2 by breaking out the dense Al_2O_3 layer, ultimately decreases the incubation period. Furthermore, Mg decreases the oxygen partial pressure at the frontier of nitridation, promoting the nitridation of Al by prohibiting the appearance of Al_2O_3 again. The content of alloy element Mg also affects the microstructure of composite. For example, AlN dispersed in the Al matrix composite with less than 1 wt% Mg, and three-dimension loose microstrucutre of AlN/Al resulted from volume nitridation of Al with higher Mg content [3].

However, Mg strongly evaporated from the alloys even at 975 °C according to the research of Rodriguez-Reyes et al. [4]. Jin et al. also found only 0.049%Mg in the alloys during the volume nitridation [5]. It seems that pre-alloy of Al and Mg is not prerequisite to the nitridation of Al, but all above researches are been trapped in Al-alloy such as Al–Mg, Al–Mg–Si, Al–Li [6, 7]. Whether can pure Al block been nitrided without alloy process? Therefore, external dopant Mg would be laid on the surface of pure Al block in order to reduce the product costs by avoiding the alloy process. In this paper, we primarily investigated the

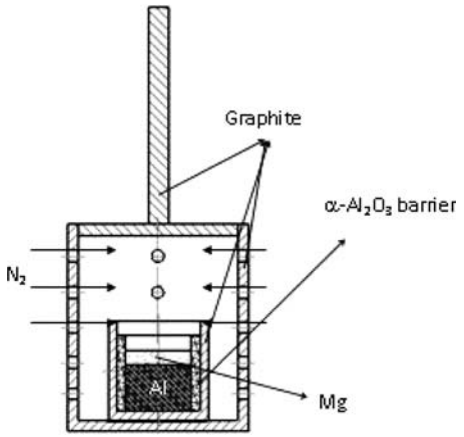

Fig. 1 Schematic diagram of the experimental setup

fabrication of AlN containing material in this modified way.

Experimental

Pure Al blocks (>99%) were set into small graphite crucible with barrier materials, and Mg (>99%) powder was covered on the surface of Al blocks. Then the small graphite crucible was settled in a hanging piece with hallow graphite cylinder, and N_2 presumably entered the cylinder from the side holes in the graphite cylinder wall, shown in Fig. 1.

The chamber was evacuated to –0.1 MPa and refilled with N_2 for three times before heating. Deeply deoxidized high pure N_2 (99.999%) gas was flowed at a rate of 10 ml/min, which simulates the stable atmosphere during the experiment. In order to avoid the entry of air into the system, the outgoing gas was bubbled through a column of water. When the furnace was heated to the set temperature 1373–1573 K at a rate of 10 °C/min, the whole assembly was put down immediately to the set temperature section and soaked for 3 h, then was cooled naturally to ambient temperature and the flowing N_2 was kept till 933 K.

The samples were weighted before and after nitridation in order to calculate the nitridation rate. X-ray Diffractometer (XRD, Philips MPD Pro) was used for powder and surface analysis. Optical microscope (OM, Zeiss Axoskop 40Apol), scanning electron microscope (SEM, Philips XL30MDP) and electron Probe Microanalyzer (EPMA, JXA8800R) were used to observe the microstructure.

Results and discussion

Figure 2a shows the weight gain change of Al block externally doping 10% Mg as a function of treating temperatures soaked in 3 h. The nitridation rate rises as the treating temperature increases, sharply especially between 1473 K and 1573 K. It reveals that higher temperature promotes the nitridation process. Although the theoretical nitridation rate of complete conversion of Al to AlN is 52%, the weight gain is only approaching 30% at 1573 K in this experiment. XRD reveals main AlN, $MgAl_2O_4$ and less Al in the as-grown powder produced at 1573 K (Fig. 3). It suggests that Al melt was not been completely transformed to AlN at all. In general, the reaction kinetic is more complex because the overall process involves not only the nitridation reaction, but also the transport of metal to the reaction frontier and the evaporation of Al (g). As shown in Fig. 2b, an Arrhenius plot is made as logarithmic growth rate ($\ln K_L$) versus the reciprocal of absolute temperature ($1/T$) and apparent activation energy of 208.7 KJ/mole was obtained by calculating the slope of the best-fit line. Yuan reported the activation energy of 20.8 KJ/mole at temperatures between 1123 K and 1473 K when Al–4Mg alloys was used and Creber et al. reported 93.7 KJ/mole when a commercial aluminum alloy, A380.1 was used [8, 9]. It is believed that the difference between these experiments may be attributed to processing parameters such as composition of Al or treating atmosphere.

The surfaces of samples treated at different temperatures were observed by SEM, shown in Fig. 4. It reveals that there are many nodules on the surfaces of all the samples.

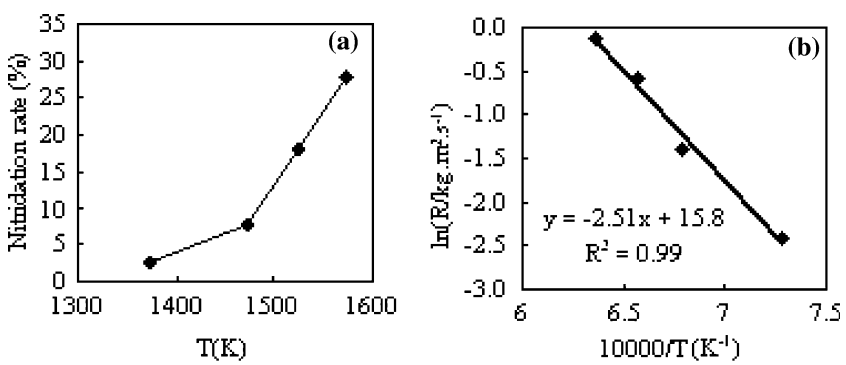

Fig. 2 Nitridation (**a**) and reaction (**b**) rates as a function of treating temperatures for Al-10%Mg at 3 h

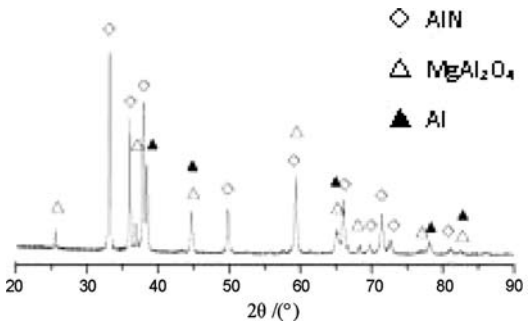

Fig. 3 XRD pattern for the powder of sample treated at 1573 K for 3 h

At 1373 K, the surface is dense and there are a few cracks, which should be attributed to the mismatch of ceramic and metal. With the increase of treating temperature, the nodules on the surface become smaller. Energy dispersive spectrometer detected Al, Mg, O and N, however XRD analysis of surface (Fig. 5) only detected AlN phase. It can be presumed there are AlN and $MgAl_2O_4$ in the surface but spinel cannot be detected due to trace content.

Along the growth direction, the samples were sectioned and polished. Figure 6 presents the microstructures observed by OM. A dense and thin AlN/Al layer (gray region) makes up of the surface at 1373 K, where metal tunnels disperse (Fig. 6b). Under the dense layer, metal phase (white region) and macro pores (dark region) predominate. It indicates only surface nitridation happened at 1373 K and transportation of melt from the bottom to the reaction frontier left caves. With elevated temperature, the reaction is more intense. According to Fig. 6c, the surface is much uneven and more macro-pores appear and metal phase is surrounded by as-grew ceramic phase. A dendrite growth of AlN/Al also was observed, shown in Fig. 6d.

Further observation on the microstructures of samples treated at different temperatures was made by SEM. At 1473 K (Fig. 7), AlN and $MgAl_2O_4$ were found in the samples, where AlN particles seem to grow out from melt but the morphology of $MgAl_2O_4$ crystals is clear. Up to 1573 K, the microstructure is relatively porous. Thick columnar AlN crystals dominate in the product and AlN whiskers also appear, shown in Fig. 8a and b. Figure 8c shows the debris of hollow Al tube, which further indicates the growth mechanism of capillary transportation [1].

As expected, the nitridation rate increases with the increase of Mg content. When the content of Mg is 1%, a negative weight gain further proves the evaporation of Al (g). Then there is a sharp increase when the content of Mg increases from 4% to 5% and the weight gain is approximately equal to that of Al block with 10 wt%Mg treated at 1573 K, indicating the critical Mg content should be higher than 4 wt% (Fig. 9a) if AlN rich matrix material will be designed.

A polished section of Al-4%Mg parallel to growth direction was observed by EPMA. Enrichment of AlN in the top part of the product was found, suggesting that the weight gain was due to the in situ formation of AlN. Figure 10 shows a typical EPMA photograph of the top part. The energy dispersive spectrometer (EDS) patterns corresponding to the regions with different hardness in Fig. 10 are shown in Fig. 11. AlN particles have higher hardness and better abrasive resistance than Al. Therefore, Al was ground and polished faster than AlN in the process of sample preparation. Further semi-quantitative analysis showed that the content of nitrogen and aluminum were about 20% and 80%, respectively. Therefore, the aggregate predominated in Fig. 10 suggests pregnant AlN particles in Al melt. As suggested by Fig. 11b, the planar region in

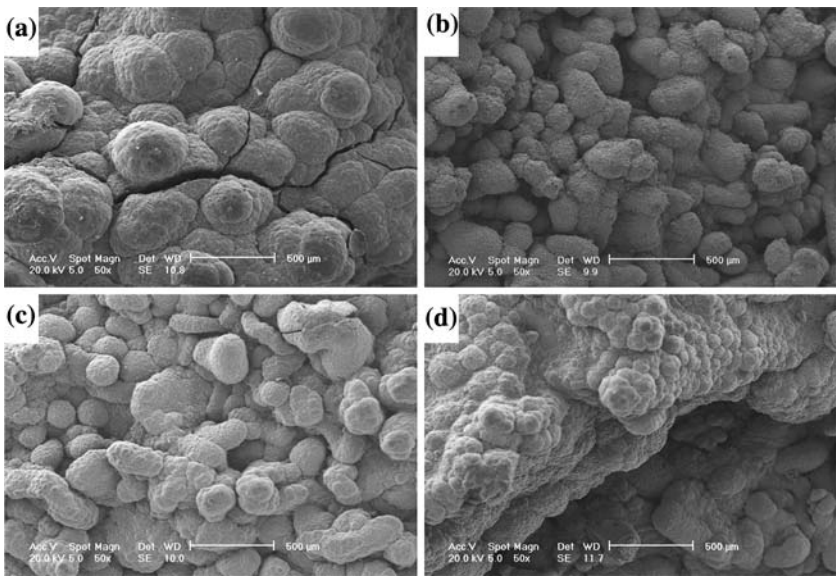

Fig. 4 Surface morphology evolution of the samples at 1373 K (**a**), 1473 K (**b**), 1523 K (**c**), and 1573 K (**d**)

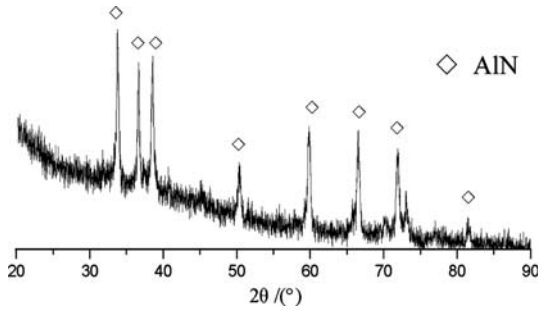

Fig. 5 XRD pattern for the surface of sample soaked at 1573 K for 3 h

Fig. 10 is pure Al. Figure 12 shows the morphology of a distinct boundary region of the top AlN–Al composite and bottom Al in the product, which also has been observed in the AlN/Al composite produced using a gas bubbling method [10]. Macro pores may be left by Al transportation to the reaction frontier, which give the free space for AlN to grow.

Conclusions

Using Mg powder as external dopant on the pure Al block, AlN/Al material has been successfully fabricated by

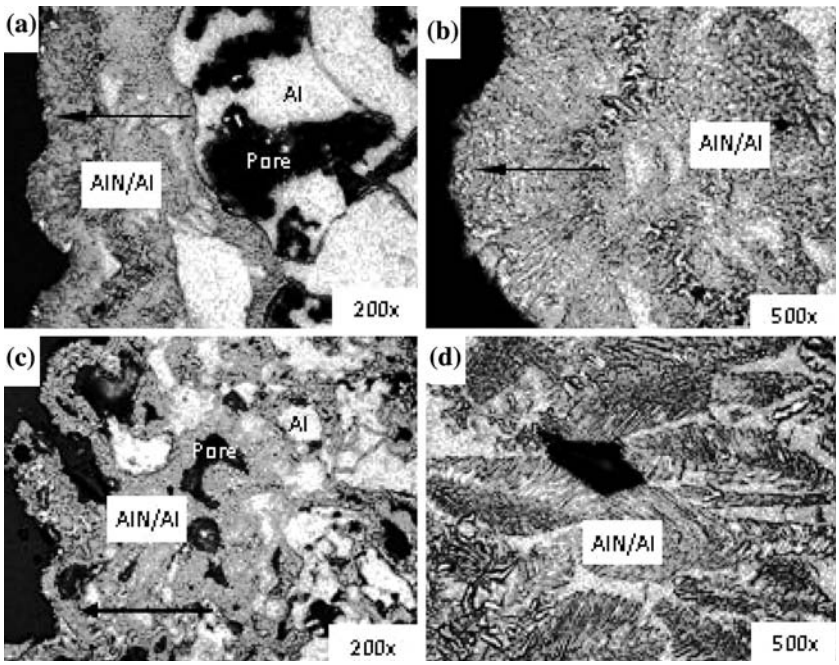

Fig. 6 Optical microstructure of samples soaked at different temperatures for 3 h (arrow shows the growth direction). (**a**, **b**) 1373 K, (**c**) 1473 K, (**d**) 1523 K

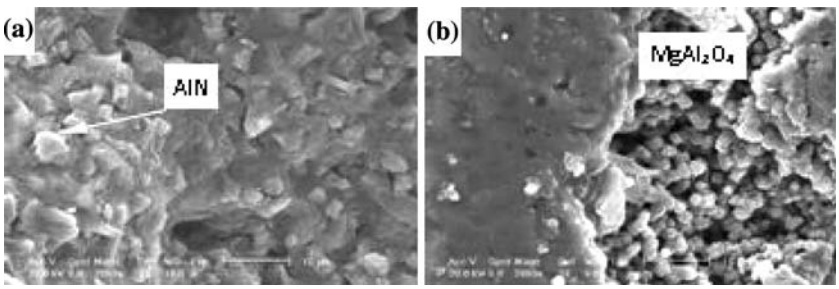

Fig. 7 SEM photographs of sample soaked at 1473 K for 3 h

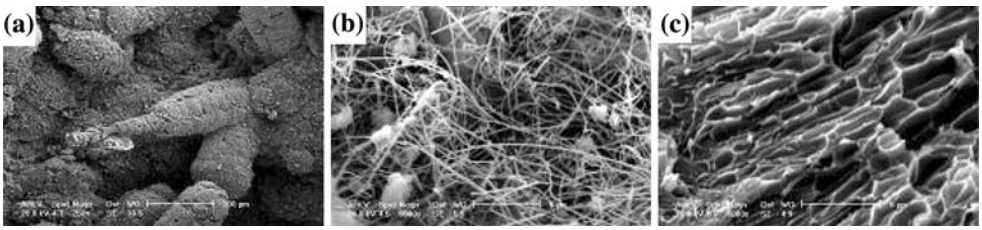

Fig. 8 SEM photographs of samples soaked at 1573 K for 3 h

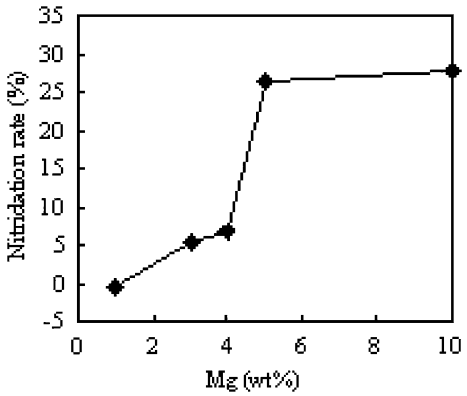

Fig. 9 Nitridation rates as a function of the content of external dopant Mg at 1573 K for 3 h

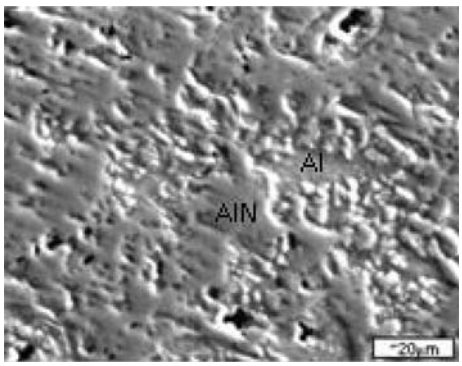

Fig. 10 EPMA images of AlN–Al composite

directed melt nitridation. Processing parameters such as treating temperature and Mg content affect the weight gain and microstructures of samples. Weight gain increases with the elevated temperature and an apparent activation energy 208.7 KJ/mole was obtained, indicating the growth of AlN controlled by chemical reaction. A lot of AlN nodules appeared on the surface and turns into smaller ones with the elevated temperature, simultaneously, the microstructure in the samples is much looser. Al rich matrix composite also can be obtained using less Mg as external

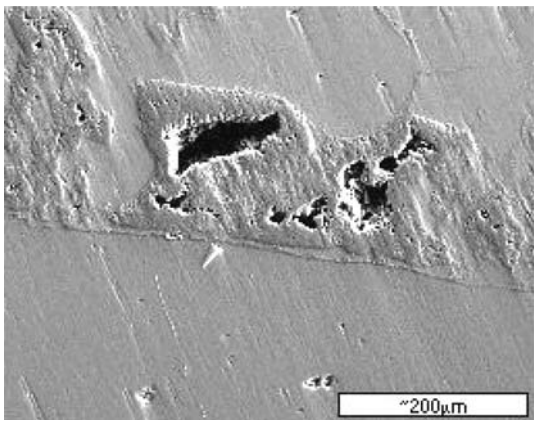

Fig. 12 EPMA image of the boundary region between the top AlN–Al composite and bottom Al

dopant. Finally, how to fabricate the required material by this modified method will be the key work in the future.

Acknowledgements We appreciate the financial supports of National Natural Science Foundation of China (50572076) and Ministry of Education of China (20040488001).

References

1. Newkirk MS, Lesher HD, Kennedy CR et al (1987) Ceram Eng Sci Proc 8(7–8):879
2. Mclachlan DR, Kuszyk JA (1996) Advances in refractories for the metallurgical industries II, Montreal, Quebec; Canada, p 237
3. Scholz H, Greil P (1991) J Mater Sci 26:669
4. Rodriguez-Reyes M, Pech-Canul MI, Parras-Medecigo EE et al (2003) Mater Lett 57:2081
5. Jin HB, Chen KX, Zhou HP et al (2000) J Inorg Mater 15(4):631 (in chinese)
6. Else B (1993) J Am Ceram Soc 76(7):1865
7. Scholz H, Greil P (1990) J Eur Ceram Soc 6:23
8. Yuan DW, Cheng VS, Yan RF et al (1994) Ceram Eng Sci Proc 15(4):85
9. Creber DK, Poste SD, Aghajanian MK et al (1988) Ceram Eng Sci Proc 9(7–8):975
10. Zheng QJ, Reddy RG (2004) J Mater Sci 39:141

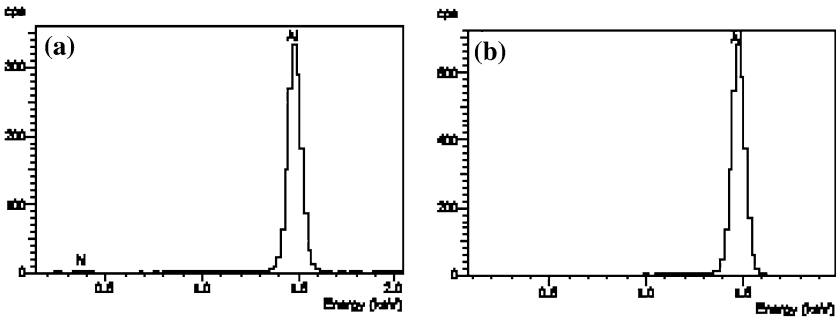

Fig. 11 EDS patterns corresponding to (**a**) aggregates and (**b**) planar region in Fig.10